

Sequential Reactions Directed by Core/Shell Catalytic Reactors

Yanhu Wei, Siowling Soh, Mario M. Apodaca, Jiwon Kim, and Bartosz A. Grzybowski*

Millimeter-sized reactor particles made of permeable polymer doped with catalysts arranged in a core/shell fashion direct sequences of chemical reactions (e.g., alkyne coupling followed by hydrogenation or hydrosilylation followed by hydrogenation). Spatial compartmentalization of catalysts coupled with the diffusion of substrates controls reaction order and avoids formation of byproducts. The experimentally observed yields of reaction sequences are reproduced by a theoretical model, which accounts for the reaction kinetics and the diffusion of the species involved.

Keywords:

- core/shell reactors
- multifunctional catalysts
- nanoparticles
- sequential reactions

1. Introduction

The ability to perform multiple reactions in one reaction vessel and in a well-defined sequence can simplify and accelerate multiple-step syntheses, and can translate into significant economic savings by reducing the amount of byproduct^[1] and by eliminating intermediate purification steps, which account for as much as 60% of the total synthetic cost.^[2] To date, most research on sequential reactions has focused on the control of intramolecular structure and reactivity in the so-called cascade (also known as tandem or domino) reactions,^[2a–c,3] on identification of compound collections suitable for multicomponent reactions^[4] (in which, however, the exact sequence of steps is rarely known^[4c,5]), and on the design of multifunctional^[2b] or modular catalysts^[6] in which reaction sequence is controlled by the arrangement of catalytic subunits.

While the elegance and practicality of many of these approaches cannot be disputed, biology teaches us that arguably a simpler strategy can be used to control reaction sequences – namely, that of spatial compartmentalization in which the consecutive reactions take place at different regions/“compartments”. It is then the transport of reaction substrates/

products between these regions that determines the outcome of the overall reaction sequence. For example, amino acids are translated into proteins in the endoplasmic reticulum (ER) but their further “packaging” takes place in the Golgi apparatus from which they later migrate to final destinations.^[7] Another manifestation of cellular compartmentalization is that of multienzyme complexes for metabolic channeling (“metabolons”)^[8] whereby biosynthetic intermediates migrate and react sequentially between catalytic sites without diffusing into the bulk of the cell.

Beyond these and other biological examples,^[6] several research groups have reported non-biological compartmentalized systems for multifunctional catalysis. One strategy that has been developed relies on the immobilization of mutually “incompatible” reagents/catalysts onto solid or macromolecular supports. For example, Avnir’s group pioneered the separate entrapment of catalysts and catalyst-poisoning reagents in sol–gel matrices, which enable the simultaneous use, in one pot, of these chemicals.^[9] This concept was demonstrated in acid–base,^[10] redox,^[11] and even enzymatic chemistries.^[12] In another approach, Hawker et al. attached acidic and basic residues to the interior of star polymers such that they did not quench each other, which allowed both acid- and base-catalyzed reactions in the same reaction vessel.^[13] Fréchet also reported a system in which “polarity-directed” sequential reactions occur in a biphasic medium comprising oil droplets suspended in aqueous phase.^[14] Spatial separation of catalysts has also been combined with system geometry, notably in the form of planar multilayer architectures. For example, Alfonso et al. fabricated two-layer MgO/PtSnAl membranes,^[15] which under constant flow carried consecutive oxidative and non-oxidative dehydrogenation of butane; on

[*] Prof. B. A. Grzybowski, Dr. Y. Wei, S. Soh, M. M. Apodaca, J. Kim
Department of Chemical and Biological Engineering
Department of Chemistry, Northwestern University
2145 Sheridan Road, Evanston, IL 60208 (USA)
E-mail: grzybor@northwestern.edu

Supporting Information is available on the WWW under <http://www.small-journal.com> or from the author.

exit, this system produced a mixture of butene isomers, butadiene, carbon monoxide, carbon dioxide, unreacted butane, and several other products. Two-layered membranes were also used in Rothenberg's cat-in-cup system,^[16] where the catalyst was immobilized on one of the membranes while the reaction substrates and products could diffuse freely in and out. In another study, Bowden et al. reported an elegant use of poly(dimethylsiloxane) (PDMS) membranes to spatially separate polar and non-polar reagents and appropriate catalysts,^[17] such that consecutive reactions could occur on different sites of the membrane. In parallel to these studies, there has been significant interest in driving sequential reactions using multifunctional/multilayered particles rather than membranes (whose incorporation into flow/diffusion systems can be cumbersome). For example, Eiser et al. synthesized Pd or Au catalytic nanoclusters surrounded by polyelectrolyte shells and suggested that these systems could be used for sequential catalysis (though only one reaction, Sonogashira cross coupling, was demonstrated).^[18] In another interesting example, Tsubaki's group described catalytic particles comprising a zeolite layer surrounding a Co/Al₂O₃ or Co/SiO₂ core.^[19] These particles were used to direct synthesis of isoparaffins from syngas, and it was suggested that upon modifications they could be used to direct sequential reactions. The last two examples suggest that while preparation of core/shell architectures is certainly feasible, the extension of these systems to sequential catalysis remains an experimental challenge requiring careful control of reaction rates versus the speed of migration of the substrates/intermediates through the supporting matrix.

In this work, we address this challenge and set out to design compartmentalized "reactor" particles, in which sequences of catalytic reactions can be controlled by the system's geometry and by the diffusion of the reagents/intermediates through the regions containing different catalysts. Specifically, we describe systems in which two catalysts (C_1 and C_2) are occluded in a permeable polymer matrix and are arranged in a core/shell manner (Figure 1a). When these composite reactors are placed in the solution containing reaction substrates, the substrates first react with C_1 (in reaction R_1) in the outer shell before diffusing to the inner core, where reaction R_2 is effected by C_2 . Provided the dimensions of the core and of the shell are appropriate, only the sequence of reactions $\{R_1, R_2\}$ takes place and the alternative sequence $\{R_2, R_1\}$ is avoided (Figure 1b). The experimentally observed yields of sequential reactions are reproduced by a theoretical model, which accounts for the reaction kinetics and the diffusion of the species involved.

2. Results and Discussion

We fabricated (see Experimental Section) and tested two types of multicomponent, core/shell reactors based on the PDMS^[20] matrix permeable to gasses (e.g., H₂, O₂, N₂, CH₄ etc.)^[21] as well as many common organic solvents^[22] including acetonitrile and toluene used in our experiments. In the first system (Figure 1b), the PDMS core contained ≈ 4.8 mM (in terms of metal atoms) of 5-nm Pd nanoparticles stabilized with dodecylamine (DDA), which are known to be efficient hydrogenation catalysts.^[23] The outer PDMS shell contained

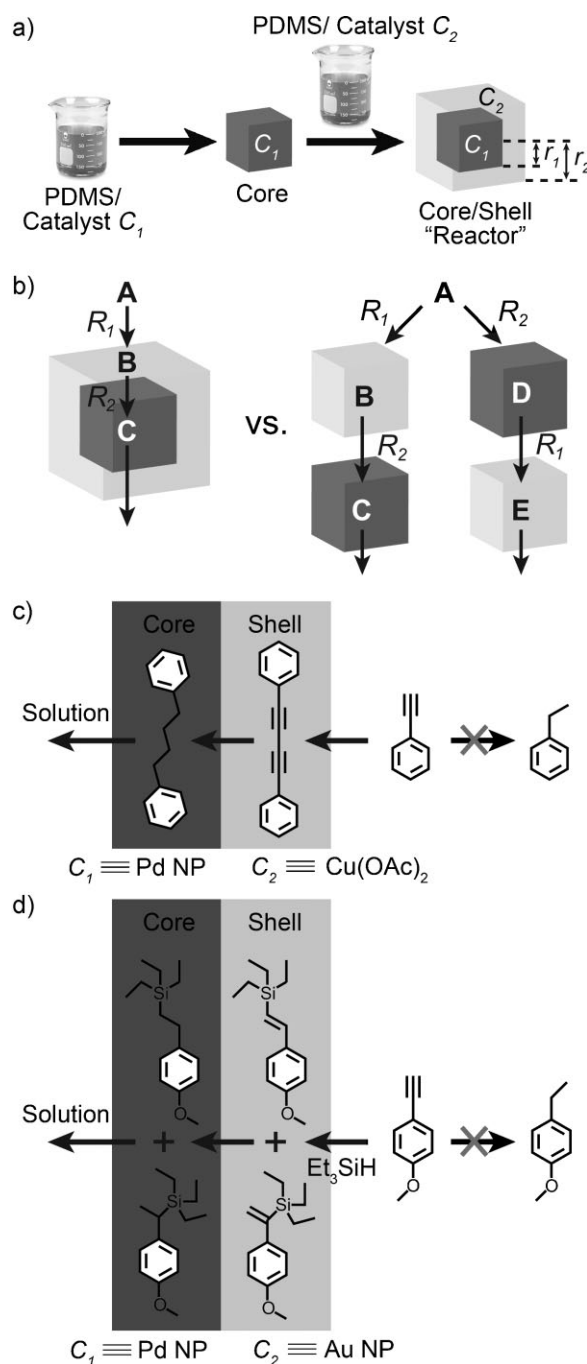


Figure 1. a) Scheme of the fabrication protocol. Cured PDMS containing catalyst C_1 is cut (using homemade precision cutter) into small cubes that are then immersed in PDMS containing catalyst C_2 . After curing, the core and shell reactors are cut into millimeter-sized cubes. b) A sequential reaction in a core/shell catalytic reactor transforms substrate A first into intermediate B (reaction catalyzed by C_1). B diffusing into the core is then converted to C (by C_2), which ultimately diffuses out of the reactor. In the absence of the core/shell architecture, as in the case of PDMS particles carrying different catalysts (right scheme), the reagents can also react first with C_2 and only then with C_1 to produce byproducts D and E. c) The species involved in the reaction sequence catalyzed by PdNP/Cu(OAc)₂ system. The core/shell architecture promotes formation of the 1,4-diphenylbutane product and prevents direct hydrogenation to phenylethane. d) Similarly, PdNP/AuNP reactors mediate hydrosilylation/hydrogenation sequence, but eliminate hydrogenation by-product (4-methoxyethylbenzene).

Table 1. Comparison of experimental and modeled steady-state distributions (molar %) of species in sequential alkyne coupling-hydrogenation reactions in PdNP/Cu(OAc)₂ reactors.

r_1 [mm]	S_t [mm]	Run #	Time [h]	Conv% _B ^[a] Exp/model	Conv% _C ^[a] Exp/model	Conv% _D ^[a] Exp/model
2	1.5	1	231	14/8.7	86/89	0.0/2.3
2	1.1	1	187	12/6.8	88/90.6	0.0/2.6
2	0.8	1	111	10/4.9	88/90.1	1.9/4.9
1.5	1.5	1	240	17/15	83/84	0.0/0.8
2	1.1	1 ^[b]	144	13	87	0.0
2	1.1	2 ^[b]	144	29	71	0.0
2	1.1	3 ^[b]	144	11	38	35

[a] The degree of conversion is calculated based on the integration of ¹H NMR signals (see Supporting Information, Section 3). [b] Experimental data from ¹H NMR integration; no theoretical data available since the concentration/aggregation of catalysis in the reused PDMS could not be quantified.

≈53 mM Cu(OAc)₂, which served as an alkyne-coupling catalyst.^[24] When the PDMS reactor was placed in acetonitrile containing a phenylacetylene substrate and under hydrogen atmosphere, this substrate was first exposed to Cu(OAc)₂ and converted to 1,4-diphenylbutadiyne before it diffused to the core where PdNPs catalyzed the hydrogenation of 1,4-diphenylbutadiyne to 1,4-diphenylbutane (Figure 1c). We emphasize that since both Cu(OAc)₂ and PdNPs are reactive towards phenylacetylene, the core/shell arrangement is essential to suppress the alternative reaction pathway leading to phenylethane. Indeed, for reactors comprising $r_1 \approx 2$ -mm cores surrounded by 1.1-mm-thick shells, the overall conversion (i.e., the yield of the two sequential reactions) to 1,4-diphenylbutane was as high as 88% (for this and other data, see Tables 1 and 2). In contrast, control experiments in which Cu(OAc)₂ and PdNPs were dispersed in separate PDMS pieces (cf. Figure 1b) or in the same PDMS piece but without any spatial ordering always gave a mixture of 1,4-diphenylbutane and phenylethane products, typically in with a ≈45:55 molar ratio.

The second system we tested comprised PdNPs occluded in the core and AuNPs in the shell regions (Figure 1d). The solvent in this case was toluene and the substrate, 4-methoxyphenylacetylene. In the presence of Et₃SiH, the shell Au particles catalyzed the conversion of this substrate into two isomers, (1-triethylsilyl-2-(4-methoxyphenyl)-ethene and 1-triethylsilyl-1-(4-methoxyphenyl)-ethene),^[25] which were then hydrogenated by PdNPs into triethyl(2-(4-methoxyphenyl)ethyl)-silane and triethyl-(1-(4-methoxyphenyl)ethyl)-silane (with a ≈5:2 molar ratio). In this case, the conversion for the reaction sequence was as high as 93% (in reactors with $r_1 \approx 2$ -mm cores and 1.8-mm-wide shells, Table 2). At the same time, no 4-methoxyethylbenzene byproducts were observed. Also, control experiments with PDMS pieces doped uniformly with both types of NP or with separate pieces containing PdNPs and AuNPs, respectively, always gave a mixture of triethyl(2-(4-methoxyphenyl)ethyl)-silane, triethyl(1-(4-methoxyphenyl)ethyl)-silane, and byproduct 4-methoxyethylbenzene, typically in a 14:6:80 molar ratio.

Table 2. Comparison of experimental and modeled steady-state distributions (molar %) of species in sequential hydrosilylation-hydrogenation reactions in PdNP/AuNP reactors.

r_1 [mm]	S_t [mm]	Run #	Time [h]	Conv% _(F1+F2) ^[a] Exp/model	Conv% _(G1+G2) ^[a] Exp/model	Conv% _H ^[a] Exp/model
2	2.7	1	23	24.6/20.3	75.4/79.6	0.0/0.1
2	1.8	1	23	7.2/11.3	92.8/88.0	0.0/0.7
2	1.8	1 ^[b]	23	7.0	93	0.0
2	1.8	1 ^[b]	23	41	59	0.0
2	1.8	1 ^[b]	23	37.5	10.4	52.1

[a] The degree of conversion is calculated based on the integration of ¹H NMR signals (see Supporting Information, Section 3), and the molar ratio of two isomer products is about 5:2. [b] Experimental data from ¹H NMR integration; no theoretical data available since the concentration/aggregation of catalysis in the reused PDMS could not be quantified.

While the yields for a single use of both types of reactor were high, the degree of conversion decreased markedly when these reactors were used multiple times (entries marked Run 1^b, 2^b, and 3^b in Tables 1 and 2). In the case of the PdNP/Cu(OAc)₂ system this was likely due to the “leaking”/diffusion of Cu(OAc)₂ out of the PDMS matrix. In the case of AuNPs, repeated swelling of the PDMS with toluene caused NP aggregation (evidenced by the color shift from red to violet^[26]) and decrease in the effective surface area of the catalytic NPs.

The parameters that control the yield of reaction sequence include concentration of catalysts occluded in PDMS, diffusivities of the various species through PDMS, and the dimensions of the reactor’s core and shell. The concentrations we used were chosen such as to load the maximal amounts of catalyst particles in PDMS while preventing – or at least minimizing – their clumping into large aggregates (this was monitored by optical microscopy or, for AuNPs, by UV/Vis spectra in which unaggregated NPs had an surface plasmon resonance (SPR) adsorption peak near 520 nm). The diffusivities are determined by the porosity of the PDMS matrix and the sizes of the diffusing species. For small molecules, the typical diffusion coefficients are $D \approx 10^{-11}$ – 10^{-10} m² s⁻¹ depending on whether PDMS is swollen by the solvent or not.^[27] For larger NPs, the diffusion coefficients are negligibly small.^[28]

The diameter of the core and the thickness of the shell offer most room for adjustment. Intuitively, for a given core size, the thicker the shell, the more complete the first of the two reactions, R_1 , should be and the less unreacted substrate should reach the core to undergo reaction R_2 therein. In other words, the thicker the shell, the higher the ratio of desired product (via the $\{R_1, R_2\}$ sequence) compared to the byproduct (via the $\{R_2, R_1\}$ sequence). Of course, this increased “selectivity” is at the expense of the time required for the $\{R_1, R_2\}$ conversion, since diffusion through thicker shell takes more time (for very thick

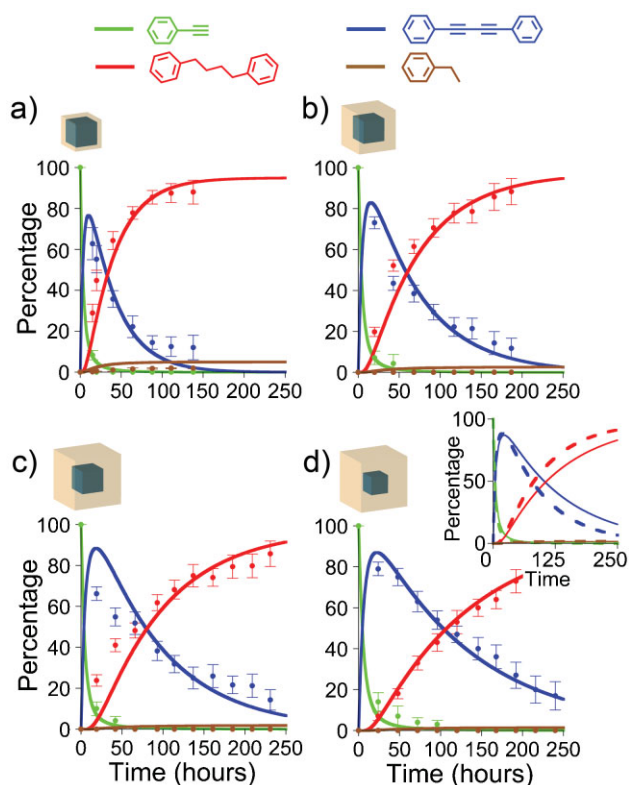


Figure 2. The composition of the reaction mixture in the PdNP/Cu(OAc)₂ system as a function of time and for different reactor dimensions. Color coding: green = phenylacetylene reactant; blue = 1,4-diphenylbutadiyne intermediate; red = the desired 1,4-diphenylbutane product, and brown = phenylethane byproduct. Markers represent experimental data determined by ¹H NMR analysis of the reaction mixture (see Supporting Information, Section 3). Error bars are based on the analysis of at least three samples for each condition. Solid lines are the predictions of the reaction-diffusion theoretical model. For (a–c) the core diameter is 4 mm but the shell thickness increases from 0.8 mm in (a), to 1.1 mm in (b), to 1.5 mm in (c). Note that for the thinnest shell (0.8 mm), the sequence goes to completion the fastest but there is a substantial amount of byproduct (brown line; also see data in Table 1). For thicker shells, the reactions reach steady state at longer times but there is less unwanted product. c,d) Compare the effects of changing core diameter (4 mm in (c) versus 3 mm in (d)) while keeping the shell thickness the same. For the smaller core, it takes longer for the reaction sequence to reach completion. This is emphasized in the inset that overlays curves from (c) (dashed lines) and those from (d) (solid lines). Other parameters used in experiments and simulations: [A]₀ = 25 mM and V_{sol} = 18 mL for shell thickness S_t = 1.5 mm; [A]₀ = 33 mM and V_{sol} = 15 mL for S_t = 1.1 mm; [A]₀ = 33 mM and V_{sol} = 10 mL for S_t = 0.8 mm. Raw experimental data for plots (a–d) are given in the Supporting Information, Section 4.

shells, the first reaction, R₁, will be complete but very little of its product will reach the core). The experimental data (by ¹H NMR, see Supporting Information, Section 3) in Tables 1 and 2 and in Figure 2a–c confirm both of these conclusions. Regarding the dimensions of the core, it is reasonable to expect that for a given shell thickness, the smaller this core is, the less time the diffusing chemicals have to complete reaction R₂ therein and the lower the yield of the {R₁, R₂} sequence is at a given reaction time. Again, these trends are confirmed by experimental data in Tables 1 and 2 and also by the plots in Figure 2c and d.

The above qualitative reasoning can be quantified by a model accounting for both the reaction and the diffusion (RD)^[29] of the species involved through the core/shell reactors. This model gives not only the steady-state concentrations at long times (cf. Tables 1 and 2) but also the timecourse of the reactions (Figure 2). Let us consider PdNP/Cu(OAc)₂ system. To simplify calculus, the reactor is approximated as a sphere (core radius r₁, overall radius r₂, shell thickness S_t = r₂ – r₁). Denoting the starting phenylacetylene as A, the 1,4-diphenylbutadiyne intermediate as B, the desired product 1,4-diphenylbutane as C, and the undesired products phenylethane as D (cf. Figure 1c), the pertinent reactions and rate constants are 2A $\xrightarrow{k_1}$ B $\xrightarrow{k_2}$ C and A $\xrightarrow{k_3}$ D. The RD equations can then be written as:

$$\frac{\partial[A]}{\partial t} = D_A \nabla^2[A] - k_1[A]^2 H_S - k_3[A] H_C \quad (1)$$

$$\frac{\partial[B]}{\partial t} = D_B \nabla^2[B] + k_1[A]^2 H_S - k_2[B] H_C \quad (2)$$

$$\frac{\partial[C]}{\partial t} = D_C \nabla^2[C] + k_2[B] H_C \quad (3)$$

$$\frac{\partial[D]}{\partial t} = D_D \nabla^2[D] + k_3[A] H_C \quad (4)$$

where square brackets denote concentrations and D_x is the diffusion coefficient of species x = A, B, C, or D. Note that because hydrogen is present in excess and its diffusivity through PDMS is ≈ 10^{–8} m² s^{–1} (roughly two to three orders of magnitude larger than of other solute species present^[21]), its partial pressure can be treated as constant and can be effectively incorporated into the apparent rate constant k₂ in Equations (2) and (3). In the reaction terms, functions H_S and H_C specify that these reactions take place in the shell and the core regions, respectively. Mathematically, H_S = H(r – r₁) and H_C = H(r) – H(r – r₁), where H(ζ) is the Heaviside step function (H(ζ) = 0 for ζ < 0, H(ζ) = 1 for ζ ≥ 0). At the surface of the cubes, r = r₂, the diffusive flux of species x across this surface is equal to the change in the concentration of x in solution around the reactor:

$$-D_x S \left. \frac{\partial[x]}{\partial r} \right|_S = \frac{\partial[x]_{sol}}{\partial t} V_{sol} \quad (5)$$

where S is the surface area of the reactor and V_{sol} is the volume of the solution per one reactor particle. The initial conditions are such that A is present outside of the cubes at some uniform concentration [A]₀ while [B]₀ = [C]₀ = [D]₀ = 0. The other model parameters are diffusion coefficients D_A ≈ D_B ≈ D_C ≈ D_D ≈ 2 × 10^{–11} m² s^{–1} for small molecules in PDMS swollen only marginally by the acetonitrile solvent^[26a] and rate constants k₁ = 0.18 s^{–1} M^{–1}, k₂ ≈ k₃ = 0.072 s^{–1} (see Supporting Information, Section 1 for more details). With these preliminaries, the equations can be solved numerically using finite difference method, implemented in Matlab R2007b.

Solid lines in Figure 2a–d plot the modeled compositions of the reaction mixture at different times and for different core/

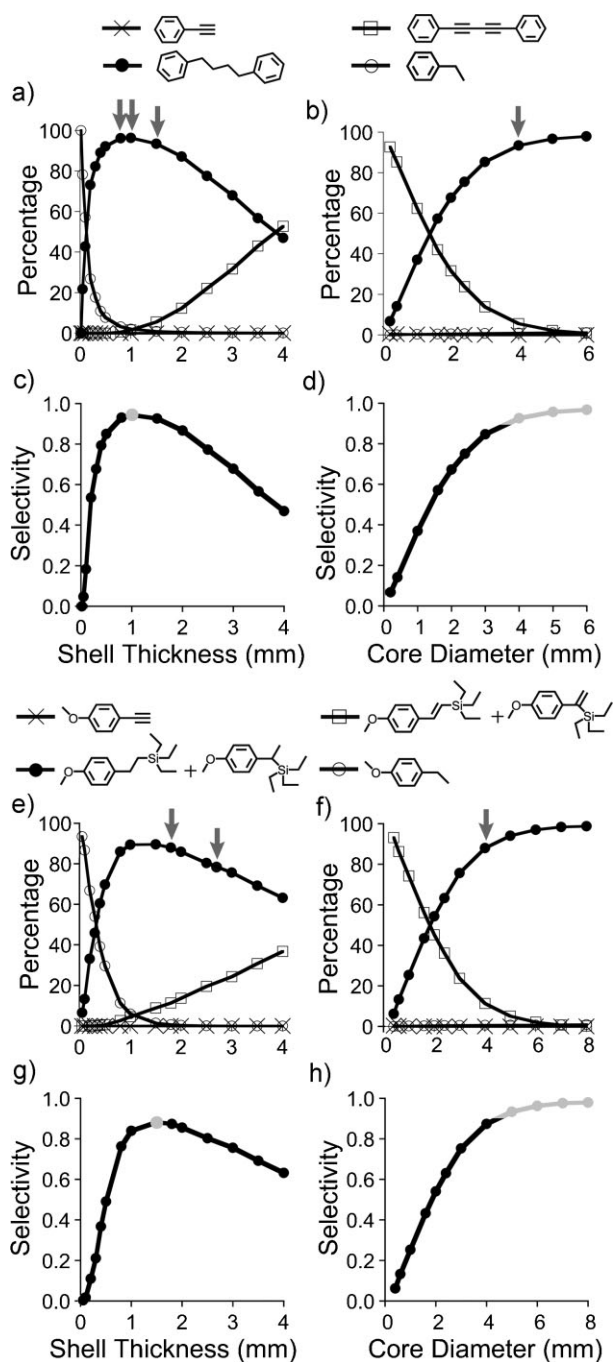


Figure 3. The effect of a) shell thickness and b) core diameter on the final (at 250 h) distribution of various species in the alkyne coupling/hydrogenation sequence catalyzed by PdNP/Cu(OAc)₂ reactors. c, d) Plots of the selectivity of desired product against byproduct (as defined in the text) with shell thickness and core diameter, respectively. Gray portions of the curves indicate the close-to-optimal dimensions for the shell and core. In (a), core diameter is kept constant at 4 mm, as in most experiments. The optimal shell thickness (i.e., one for which the desired 1,4-diphenylbutane to side phenylethane products is maximal) is around 1 mm, as shown in (c) (compare with Table 1). In (b), the shell thickness is kept constant at 1.5 mm, and the optimal core diameter as shown in (d) is above 3.5 mm, as in experiments. The arrows indicate conditions used in experiments. e–h) Similar plots for the PdNP/AuNP reactors at 23 h. In (e), core diameter is kept constant at 4 mm, and the optimal shell thickness in (g) is around 1.5 mm. In (f), shell thickness is kept constant at 1.8 mm and the optimal shell thickness is above ≈4.5 mm.

shell dimensions. These modeled dependencies agree well with the experimental data indicated by solid markers. It is worth emphasizing that this agreement is achieved with no free/fitting parameters but only physical quantities determined experimentally (see also Supporting Information, Section 1). Of course, the modeled dependencies confirm the experimental trends discussed earlier (better selectivity but slower conversion for thicker shells; higher degree of conversion with larger cores).

Another significant conclusion from the model is that it can be used to estimate the “optimal” core diameters and/or shell thicknesses for which the selectivity (here, ratio of the desired products to byproducts, normalized to 1) is maximal. This is illustrated in Figure 3 where the gray portions in the selectivity plots indicate the core diameters maximizing the selectivity, and shell thicknesses for which selectivities are above 0.9. The arrows in the corresponding concentration plots indicate the actual dimensions in our experiments – as can be seen, the reactors we used had dimensions close to the optimal values predicted theoretically.

Finally, we note that the model is applicable to both the PdNP/Cu(OAc)₂ and PdNP/AuNP systems. In the latter case, the RD equations have to be modified to account for the fact that the reactions in the shell involve both 4-methoxyphenylacetylene and Et₃SiH. With appropriate values of diffusion and rate constants (for details see Supporting Information, Section 2), the model reproduces the experimental distribution of intermediates and products (Table 2).

3. Conclusions

In summary, we have demonstrated control of sequential reactions with core/shell catalytic reactors. The principle of compartmentalization underlying this work appears general and can be extended to other types of sequential-reaction systems, in which reaction centers are spatially disjoint but are “coupled” by the transport of chemicals involved. Reaction-diffusion modeling provides an accurate mathematical tool with which to study and design such systems. The practical problem to be solved is the decrease of catalytic activity when reactors due to the leaking or aggregation of the catalysts when the reactors are reused multiple times; these problems could potentially be avoided either by the use of supporting matrices that limit diffusion (e.g., mesoporous aerogels of zeolites for NP catalysts) or by covalent immobilization of the catalysts on the polymer matrix.

4. Experimental Section

Synthesis of Pd Nanoparticles: i) 2-nm Pd NP seeds: 0.1 mmol palladium acetate, Pd(OAc)₂, was dissolved by sonication (≈10 min) in a toluene solution (13.4 mL) of DDA (2.1 mmol) and dodecyltrimethylammonium bromide (DDAB, 1.1 mmol). In a separate vial, a solution of tetrabutylammonium borohydride (TBAB, 0.7 mmol), DDAB (0.2 mmol), and toluene (4.9 mL) was prepared by sonication. The two solutions were mixed and stirred

overnight at room temperature to generate 2-nm Pd NP seeds. ii) 5 nm Pd NPs: Pd(OAc)₂ (0.5 mmol) was dissolved by sonication in a toluene solution (67 mL) of DDA (10.7 mmol), and DDAB (5.3 mmol). To this solution the seed solution described above was added. In a separate vial, a solution of DDAB (2.1 mmol) and toluene (21 mL) in anhydrous hydrazine (4.2 mmol) was prepared by sonication. The hydrazine solution was added dropwise (over ≈30 min) to the palladium solution and then stirred at room temperature overnight to generate ≈5-nm Pd NPs.

Reactor fabrication: Pd NPs were precipitated from toluene by the addition of methanol and were then redispersed in hexane. PdNP/hexane solution was mixed into PDMS (Sylgard 184, Dow Chemicals) prepolymer and crosslinker, followed by degassing and curing in an oven at 70 °C overnight. After curing, the PDMS was cut into blocks of dimensions ≈4 × 4 × 4 mm³. The PdNP-containing PDMS cubes were immersed into a mixture of PDMS prepolymer, crosslinker, and Cu(OAc)₂ dissolved in THF (or AuNPs in dichloromethane). This mixture was then degassed and cured in an oven at 70 °C overnight. Afterwards, the PDMS slab was cut (using a homemade precision cutter) around the immersed PdNP cores to give approximately cubic core/shell reactors (see Figure 1d).

Sequential alkyne coupling-hydrogenation reactions: The PDMS reactors comprised a core containing PdNPs (≈4.8 nm by Pd atoms) and a shell containing Cu(OAc)₂ (≈53 nm). Such reactors (typically ≈50) were placed in a flask containing phenylacetylene substrate in CH₃CN (the specific concentrations differ for reactors of different dimensions and are given in the main text), followed by stirring at room temperature and under hydrogen atmosphere for up to 10 days. Every 12–24 h a small aliquot of the reaction mixture was withdrawn using a syringe and analyzed by 400 MHz ¹H NMR (in CDCl₃). When the distribution of products reached steady state, the reactors were removed, the solvent was evaporated, and the products were purified by column chromatography (silica, hexane). The spectra were i) for 1,4-diphenylbutadiyne, ¹H NMR (400MHz, CDCl₃, δ): 7.56 (d, 2H), 7.38 (m, 3H); ¹³C NMR (400MHz, CDCl₃, δ): 132.7, 129.4, 128.6, 122.1, 81.8, 74.2., ii) for 1,4-diphenylbutane, ¹H NMR (400MHz, CDCl₃, δ): 7.22 (d, 2H), 7.14 (m, 3H), 2.6 (t, 2H), 1.63 (t, 2H); ¹³C NMR (400MHz, CDCl₃, δ): 128.6, 128.5, 125.9, 31.8, 22.9.

Sequential hydrosilylation–hydrogenation reactions: In a typical procedure, the core of the PDMS reactors was loaded with PdNPs (≈4.8 nm by Pd atoms) and the shell with AuNPs (≈3.5 nm by Au atoms). A flask containing ≈50–120 PdNP/AuNP core/shell cubes was dried by gas flame and cooled under Ar. To this dry flask was added 40 mL of dry toluene, followed by the addition of 0.3 mmol 4-methoxyphenylacetylene and 0.45 mmol of triethylsilane. The reaction mixture was heated to 75 °C under hydrogen atmosphere for up to 23 hours. Upon completion, the solution was drawn out by syringe and the reactors were washed with 3 × 30 mL CH₂Cl₂. The crude products were obtained by combining all organic solution and evaporating solvent under vacuum. The products containing two isomers (triethyl(2-(4-methoxyphenyl)ethyl)-silane and triethyl(1-(4-methoxyphenyl)ethyl)-silane in a ≈5:2 molar ratio) were purified by column chromatography (silica, 10% dichloromethane in hexane). Spectral characterization triethyl(2-(4-methoxyphenyl)ethyl)-silane, ¹H NMR (400MHz, CDCl₃, δ): 7.08 (d, 2H), 6.79 (d, 2H), 3.76 (s, 3H), 2.53 (m, 2H), 0.90 (t, 9H), 0.83 (m, 2H), 0.52 (q, 6H); ¹³C NMR (400MHz, CDCl₃,

δ): 128.7, 113.9, 55.5, 29.3, 14.0, 7.7, 3.4. Triethyl(1-(4-methoxyphenyl)ethyl)-silane, ¹H NMR (400MHz, CDCl₃, δ): 6.95 (d, 2H), 6.76 (d, 2H), 2.21 (q, 1H), 1.31 (d, 3H), 0.80 (m, 9H), 0.46 (q, 6H). ¹³C NMR (400MHz, CDCl₃, δ): 128.0, 113.7, 55.5, 25.8, 15.9, 7.7, 2.2.

Acknowledgements

This work was supported by the Non-equilibrium Energy Research Center (NERC), which is an Energy Frontier Research Center funded by the U.S. Department of Energy, Office of Science, Office of Basic Energy Sciences under Award Number DE-SC0000989.

- a) L. F. Tietze, *Chem. Rev.* **1996**, *96*, 115; b) J. Shin, H. Matsushima, J. W. Chan, C. E. Hoyle, *Macromolecules* **2009**, *42*, 3294; c) R. A. Bunce, *Tetrahedron* **1995**, *51*, 13103.
- a) J. Lee, Y. Na, H. Han, S. Chang, *Chem. Soc. Rev.* **2004**, *33*, 302; b) F. X. Felpin, E. Fouquet, *ChemSusChem* **2008**, *1*, 718; c) J. C. Wasilke, S. J. Obrey, R. T. Baker, G. C. Bazan, *Chem. Rev.* **2005**, *105*, 1001; d) Y. Hong, W. Hong, H. N. Chang, *Biotech. Lett.* **2000**, *22*, 871.
- a) N. Hall, *Science* **1994**, *266*, 32; b) J. Barluenga, A. Dieguez, A. Fernandez, F. Rodriguez, F. J. Fananas, *Angew. Chem.* **2006**, *118*, 2145; *Angew. Chem. Int. Ed.* **2006**, *45*, 2091; c) N. Nishibayashi, M. Yoshikawa, Y. Inada, M. Hidai, S. Uemura, *J. Am. Chem. Soc.* **2004**, *126*, 16066; d) W. J. Zuercher, M. Hashimoto, R. H. Grubbs, *J. Am. Chem. Soc.* **1996**, *118*, 6634.
- a) B. A. Seigal, C. Fajardo, M. L. Snapper, *J. Am. Chem. Soc.* **2005**, *127*, 16329; b) A. Pinto, L. Neuville, P. Retailleau, J. Zhu, *Org. Lett.* **2006**, *8*, 4927; c) D. Enders, M. R. M. Hüttl, C. Grondal, G. Raabe, *Nature* **2006**, *441*, 861.
- a) M. Rueping, A. Kuenkel, F. Tato, J. W. Bats, *Angew. Chem.* **2009**, *121*, 3754; *Angew. Chem. Int. Ed.* **2009**, *48*, 3699; b) A. Padwa, S. K. Bur, *Tetrahedron* **2007**, *63*, 5341.
- a) C. Khosla, *AIChE Journal* **2009**, *55*, 1926; b) C. M. Kao, M. McPherson, R. N. McDaniel, H. Fu, D. E. Cane, C. Khosla, *J. Am. Chem. Soc.* **1998**, *120*, 2478.
- H. Lodish, A. Berk, P. Matsudaira, C. A. Kaiser, M. Krieger, M. P. Scott, S. L. Zipursky, J. Darnell, *Molecular Cell Biology*, 5th ed., W.H. Freeman and Company, New York **2004**.
- a) P. A. Srere, *Annu. Rev. Biochem.* **1987**, *56*, 89; b) B. S. J. Winkel, *Annu. Rev. Plant Biol.* **2004**, *55*, 85; c) P. V. Reddy, A. B. Pardee, *Proc. Natl. Acad. Sci. USA* **1980**, *77*, 331.
- F. Gelman, J. Blum, D. Avnir, *J. Am. Chem. Soc.* **2000**, *122*, 11999.
- F. Gelman, J. Blum, D. Avnir, *Angew. Chem.* **2001**, *113*, 3759; *Angew. Chem. Int. Ed.* **2001**, *40*, 3647.
- F. Gelman, J. Blum, D. Avnir, *New J. Chem.* **2003**, *27*, 205.
- F. Gelman, J. Blum, D. Avnir, *J. Am. Chem. Soc.* **2002**, *124*, 14460–14463.
- B. Helms, S. J. Guillaudeu, Y. Xie, M. McMurdo, C. J. Hawker, J. M. J. Fréchet, *Angew. Chem. Int. Ed.* **2005**, *44*, 6384; *Angew. Chem.* **2005**, *117*, 6542.
- S. T. Scroggins, Y. Chi, J. M. J. Fréchet, *Angew. Chem. Int. Ed.* **2009**. DOI: 10.1002/anie.200902945.
- M. J. Alfonso, M. Mene'ndez, J. Santamaria, *Ind. Eng. Chem. Res.* **2001**, *40*, 1058.
- A. V. Gaikwad, V. Boffa, J. E. ten Elshof, G. Rothenberg, *Angew. Chem.* **2008**, *120*, 5487; *Angew. Chem. Int. Ed.* **2008**, *47*, 5407.

- [17] a) M. B. Runge, M. T. Mwangi, A. L. Miller, II, M. Perring, N. B. Bowden, *Angew. Chem.* **2008**, *120*, 949; *Angew. Chem. Int. Ed.* **2008**, *47*, 935; b) A. L. Miller, N. B. Bowden, *J. Org. Chem.* **2009**, *74*, 4834.
- [18] D. H. Turkenburg, A. A. Antipov, M. B. Thathagar, G. Rothenberg, G. B. Sukhorukov, E. Eiser, *Phys. Chem. Chem. Phys.* **2005**, *7*, 2237.
- [19] a) J. Bao, J. He, Y. Zhang, Y. Yoneyama, N. Tsubaki, *Angew. Chem.* **2008**, *120*, 359; *Angew. Chem. Int. Ed.* **2008**, *47*, 353; b) J. He, Z. Liu, Y. Yoneyama, N. Nishiyama, N. Tsubaki, *Chem. Eur. J.* **2006**, *12*, 8296.
- [20] M. T. Mwangi, M. B. Runge, N. B. Bowden, *J. Am. Chem. Soc.* **2006**, *128*, 14434.
- [21] T. C. Merkel, V. I. Bondar, K. Nagal, B. D. Freeman, I. Pinna, *J. Polym. Sci.: Polym. Phys.* **2000**, *38*, 415.
- [22] J. N. Lee, C. Park, G. M. Whitesides, *Anal. Chem.* **2003**, *75*, 6544.
- [23] a) L. Wu, B. L. Li, Y. Y. Huang, H. F. Zhou, Y. M. He, Q. H. Fan, *Org. Lett.* **2006**, *8*, 3605; b) J. Alvarez, J. Liu, E. Roman, A. E. Kaifer, *Chem. Commun.* **2000**, 1151.
- [24] P. Siemsen, R. C. Livingston, F. Diederich, *Angew. Chem.* **2000**, *112*, 2740; *Angew. Chem. Int. Ed.* **2000**, *39*, 2632.
- [25] A. M. Caporusso, L. A. Aronica, E. Schiavi, G. Martra, G. Vitulli, P. Salvadori, *J. Organometallic Chemistry* **2005**, *690*, 1063.
- [26] a) R. Klajn, K. J. M. Bishop, M. Fialkowski, M. Paszewski, C. J. Campbell, T. P. Gray, B. A. Grzybowski, *Science* **2007**, *316*, 261; b) R. Klajn, P. J. Wesson, K. J. M. Bishop, B. A. Grzybowski, *Angew. Chem.* **2009**, *121*, 7169; *Angew. Chem. Int. Ed.* **2009**, *48*, 1.
- [27] a) M. M. Santore, M. J. Kaufman, *J. Polym. Sci. Polym. Phys.* **1996**, *34*, 1555; b) J. P. Robinson, E. S. Tarleton, K. Ebert, C. R. Millington, A. Nijmeijer, *Ind. Eng. Chem. Res.* **2005**, *44*, 3238; c) T. Hajsz, I. Csetneki, G. Filipcsei, M. Zrinyi, *Phys. Chem. Chem. Phys.* **2006**, *8*, 977.
- [28] a) D. H. Cole, K. R. Shull, P. Baldo, L. Rehn, *Macromolecules* **1999**, *32*, 771; b) D. H. Cole, K. R. Shull, L. E. Rehn, P. M. Baldo, *Nucl. Instrum. Methods Phys. Res. Sect. B* **1997**, 283.
- [29] a) B. A. Grzybowski, *Chemistry in Motion: Reaction Diffusion Systems for Micro and Nanotechnology*, Wiley, Chichester, UK **2009**; b) W. M. Deen, *Analysis of Transport Phenomena*, Oxford University Press, New York **1998**.

Received: December 16, 2009
Published online: March 1, 2010